CARBON 66 (2014) 340–350

Available at www.sciencedirect.com

ScienceDirect

journal homepage: www.elsevier.com/locate/carbon

Single stage electrochemical exfoliation method for the production of few-layer graphene *via* intercalation of tetraalkylammonium cations ☆

Adam J. Cooper [a], *Neil R. Wilson* [b], *Ian A. Kinloch* [c], *Robert A.W. Dryfe* [a,*]

[a] *School of Chemistry, University of Manchester, Oxford Road, Manchester M13 9PL, UK*
[b] *Department of Physics, University of Warwick, Gibbet Hill Road, Coventry CV4 7AL, UK*
[c] *School of Materials, University of Manchester, Oxford Road, Manchester M13 9PL, UK*

ARTICLE INFO

Article history:
Received 29 April 2013
Accepted 4 September 2013
Available online 11 September 2013

ABSTRACT

We present a non-oxidative production route to few layer graphene *via* the electrochemical intercalation of tetraalkylammonium cations into pristine graphite. Two forms of graphite have been studied as the source material with each yielding a slightly different result. Highly orientated pyrolytic graphite (HOPG) offers greater advantages in terms of the exfoliate size but the source electrode set up introduces difficulties to the procedure and requires the use of sonication. Using a graphite rod electrode, few layer graphene flakes (2 nm thickness) are formed directly although the flake diameters from this source are typically small (*ca.* 100–200 nm). Significantly, for a solvent based route, the graphite rod does not require ultrasonication or any secondary physical processing of the resulting dispersion. Flakes have been characterized using Raman spectroscopy, atomic force microscopy (AFM) and X-ray photoelectron spectroscopy (XPS).

1. Introduction

Graphene, with its honeycomb lattice consisting entirely of sp^2 carbon hybridisation, possesses exceptional electronic and mechanical characteristics. As well as monolayer, AB stacked bi-layer and tri-layer graphene have also attracted major interest and display desirable properties for applications in electronics [1] and composites [2] in particular.

Since the first report of monolayer graphene by Geim, Novoselov and co-workers [3] in 2004, isolated *via* the "scotch tape" method, there have been sustained efforts to find a scalable, high yield and high purity production method for graphene. There are currently two accepted approaches to the "bottom up" production of graphene. The first is *via* growth from a small molecular carbon source, such as chemical vapour deposition (CVD) on a catalytic metal surface, or *via* epitaxial growth from silicon carbide (SiC). The advantage of the "bottom up" approaches is that large areas of graphene are potentially obtainable. Epitaxial growth offers a limited selection of substrates however, and the graphene film cannot readily be transferred from the growth substrate. CVD provides advantages in this respect, since recent work has shown success in transferring CVD graphene to various substrates [4–6]. CVD graphene however is rarely defect free, and the quality of the film is often inferior to mechanically cleaved graphene, since the electronic quality of graphene is heavily dependent on the presence of grain boundaries within the films. Additionally, with respect to bi-layer and tri-layer

* *Corresponding author:* Fax: +44 1612754598.
E-mail address: robert.dryfe@manchester.ac.uk (R.A.W. Dryfe).

0008-6223/$ - see front matter
http://dx.doi.org/10.1016/j.carbon.2013.09.009

materials, CVD and SiC graphene films tend to be turbostratic and thus the divergence from AB stacking results in significant loss of the unique advantages derived from the structure of the AB stacked materials [7,8]. Perhaps most significantly, the comparatively high costs associated with CVD growth of high quality graphene currently make the route unfeasible for large scale industrial synthesis [9].

The alternative route to graphene production is *via* the exfoliation of a bulk graphite source, as exemplified by the original micromechanical cleavage of high quality graphite samples. A scalable analogue of this approach focuses on solution phase exfoliation of highly ordered and defect free graphite, which also allows for potential chemical functionalisation if desired.

The solution phase methods generally involve the production of graphene oxide (GO), either by acid exfoliation such as the Hummers method or by electrochemical oxidative exfoliation of bulk graphite, followed by chemical reduction of the intermediate GO products [10]. It has been shown that successful graphene exfoliation occurs *via* the GO route, one reason being the relative ease of the technique [11]. The oxygen containing functional groups formed within the graphene sheets facilitate the dispersion of the sheets in aqueous and organic solvents leading to increased yields of exfoliate. However these oxygen containing functional groups reduce graphene's electronic conductivity, which cannot be completely restored upon further chemical reduction thereby losing the inherent advantages of monolayer graphene [12–14].

Sonication in organic solvents is another plausible route to graphene production [15], although its disadvantages include low yields and the large amount of energy associated with any scale-up of the process. Consequently, a scalable non-oxidative method of graphene production is becoming increasingly desirable.

It has been shown that stable graphene dispersions can be formed *via* the (non-electrochemical) intercalation of halogen compounds followed by various annealing/sonication processes. The different molecular dimensions of ICl and IBr were shown to induce stage-selectivity of the intercalant, thus leading to controlled bi-layer and tri-layer dispersions, respectively [1].

Both anions and cations are known to intercalate effectively between the graphene layers in bulk forms of graphite. It has so far been reported that anionic intercalation successfully leads to the exfoliation of the graphite anode. However, due to the positive potentials required for anionic exfoliation, this method generally results in functionalised graphene sheets [11,14,16–22].

The alternative is cationic intercalation, with or without electrochemical control, which would avoid the formation of oxidised products, since negative potentials would be required for the intercalation. Although lithium intercalation into graphite electrodes is a very well-studied process, because of the development of lithium-ion battery technology, the focus of prior research has been on the prevention of any electrode expansion/exfoliation primarily to increase battery cycle life [23]. Work by Simonet and co-workers from the late 1970s describe graphitic electrode expansion work driven by the intercalation of tetraalkylammonium cations [24,25]. However, in these articles there is no indication of graphite exfoliation or the subsequent production of graphene.

Much more recently, Sirisaksoontorn et al. [22] have shown that tetrabutylammonium (TBA) can be chemically intercalated into graphitic carbon and is thereby stabilized by the formation of a graphite intercalation complex (GIC). It should be noted that these GICs were formed *via* the displacement reaction of TBA cations and a sodium-ethylenediamine complex, not *via* controlled electrochemical intercalation. However the authors of the work state that the intercalated TBA ion separates the graphite layers by 0.467 nm, a comparable separation to TBA intercalation in montmorillonite (0.49 nm) and molybdenum disulphide (MoS_2) (0.52 nm) [26,27]. Electrochemical intercalation is a more controlled route for the formation of GICs and enables the intercalated species to be de-intercalated with relative ease [28–30].

Wang et al. have used cationic intercalation as a pre-treatment to graphite exfoliation [14]. They show exfoliation of graphite into few-layer graphene flakes *via* the intercalation of Li^+ complexes and subsequent sonication of the intercalated compound. Two issues of concern are the extreme potentials (-15 ± 5 V) and sonication stage required for exfoliation of the expanded graphite. Other work also looks at a cathodic pre-treatment stage but work remains to remove the required sonication step from the process [19,31].

In summary, it is desirable to develop a scalable, high yield single stage exfoliation route to single layer graphene. We present an electrochemical intercalation route, which can yield graphene directly *via* the intercalation of tetraalkylammonium cations, avoiding the sonication process for certain types of graphite source. Contrast is made with the use of HOPG electrodes, where a secondary sonication process was found to be necessary. Significantly, the route presented avoids the formation of GO thus omitting the undesirable chemical reduction stage to obtain graphene.

2. Experimental

2.1. Methods and materials

HOPG (SPI-2 grade, $10 \times 10 \times 1$ mm) was obtained from SPI supplies (West Chester, PA, USA). The following chemicals were ordered from Sigma–Aldrich and used without further purification: 1-methyl-2-pyrrolidone (NMP, biotech. grade $\geqslant$ 99.00%), lithium tetrafluoroborate ($LiBF_4$, 99.99%), tetramethylammonium perchlorate ($TMAClO_4$, 99.99%), tetraethylammonium tetrafluoroborate ($TEABF_4$, 99.99%) and tetrabutylammonium tetrafluoroborate ($TBABF_4$, 99.99%). "Anodisc" 13 mm Alumina membranes (0.02 μm pore size) were supplied by Whatman (Maidstone, UK).

Electrode materials and cells: as illustrated in Fig. S1 (Supporting information), two types of working electrode (HOPG and a graphite rod) were employed in the 3-electrode system, which also consisted of a platinum wire counter electrode and silver wire (with glass frit) or platinum wire as the pseudo-reference electrode. However, to facilitate comparison with other work, all potentials are quoted with respect to a $Ag/AgClO_4$ reference electrode, constructed by placing a silver wire in a solution of 0.01 M $AgClO_4$ and 0.1 M $TBAClO_4$ in NMP.

The reference solution is separated from the bulk electrolyte by a glass frit (Vycor®, Scientific and Medical Products Ltd., Cheadle, UK) and sealed *via* heat shrink. For reference, the potential of the ferrocene couple ($FeCp_2/FeCp_2^+$) in NMP was found to be 0.428 V vs. $Ag/AgClO_4$. Tetraalkylammonium cations were chosen as the intercalating species. Tetramethylammonium perchlorate (TMA ClO_4), tetraethylammonium tetrafluoroborate (TEA BF_4), and tetrabutylammonium tetrafluoroborate (TBA BF_4), were employed as electrolytes. The electrolyte (0.1 M) was dissolved in NMP (10 mL) in a 3-neck round bottom flask. All potentials were controlled by a PGSTAT100 potentiostat (Autolab, Utrecht, The Netherlands) using Autolab GPES software. All solutions were saturated with argon for *ca.* 20 min prior to electrochemical treatment and analysis.

Voltammetry was performed using a scan rate of 0.1 V s^{-1} in all cases. The potentials observed in the cyclic voltammetry (CV) were used to define those set in chronoamperometric mode to control the intercalation processes. Following electrochemical intercalation, the expanded HOPG was removed and sonicated (Elma ELMASONIC P70H) in pure NMP (10 mL) at approximately 100 W for a range of times (between 1 min and 12 h). Electrochemical cell temperatures were controlled *via* a Grant GD100 water bath. Sonicated samples were then centrifuged (SIGMA 2–16, SIGMA Laborzentrifugen, Osterode am Harz, Germany) at 13,500 rpm for 30 min and the supernatant decanted and left to stand in a separate sample vial for 24 h. From this dispersion, a 2 mL aliquot was filtered through the "Anodisc" alumina membranes. The exfoliation products remaining on the membranes were washed with acetone and air dried before being directly analysed *via* Raman spectroscopy using a 633 nm excitation wavelength (Renishaw RL633 Class 3B 20 mW HeNe laser) at 10% intensity. The Raman spectrometer was a Renishaw Mk1 System 2000 RM fitted with an Olympus BH2 microscope.

XPS data was collected on a Thermo Scientific K-Alpha spectrometer, using a monochromatic AlKα X-ray source operated at 100 W. The analysis area was 300 μm^2 and charge neutralisation was used for all analysis.

For all graphite rod experiments, the exfoliate dispersion was removed and left to settle for 48 h. The supernatant was decanted and placed in a separate vial. Of this dispersion, a 2 mL aliquot was removed, filtered and analysed *via* Raman spectroscopy and AFM. For AFM measurements, and subsequent Raman analysis, a 1 mL aliquot of the supernatant was removed and pipetted onto oxidised silicon (Si/SiO_2) wafers pre-heated to *ca.* 200 °C. The solvent was removed *via* evaporation in a vacuum oven and the wafer washed with acetone to remove any residual electrolyte. The silicon substrates and exfoliate were left to dry in air for 1 h prior to AFM analysis, which was conducted on an Asylum Research MFP3D-SA microscope.

3. Results

3.1. *Preliminary HOPG cyclic voltammetry (CV)*

NMP has been chosen as the intercalating solvent for this study because it has previously been found to disperse graphene readily in sonication experiments [15]. NMP is also an excellent solvent for electrochemical investigations due to its large accessible potential window and relatively low toxicity [32].

$LiBF_4$ was used as the initial electrolyte in NMP (10 mL). The applied potential of the HOPG working electrode ($3 \times 10 \times 0.5$ mm) was swept between 0.0 V and −6.0 V using CV (Fig. 1a).

Scanning from 0 to −6 V resulted in a clear cathodic peak current associated with the intercalation of Li^+ into the graphite electrode. Subsequently, on the reverse scan an anodic peak current is observed which is associated with the de-intercalation of Li^+, following its intercalation between the layers of HOPG [33,34]. This intercalation/de-intercalation process is a very well known, structurally reversible process. No visible expansion was observed for the HOPG electrode, which is consistent with the crystallographic diameter of Li^+ (0.146 nm), being smaller than the HOPG interlayer spacing (0.354 nm) [35,36]. Successive scans did yield a steady decrease in the peak currents, which we attribute to solvent/electrolyte breakdown at large negative potentials, noting that the experiments were not performed in an environment where water and oxygen where rigorously excluded. Additionally, the intercalation peak at *ca.* −5 V can be seen to shift to more positive potentials on successive scanning and eventually settles at *ca.* −4 V. It was possible to obtain repeatable voltammetric scans (Fig. 1b) by scanning over a smaller potential range to ensure a lesser degree of intercalation/de-intercalation and thereby minimizing the effects of electrolyte decomposition.

The same experiments were repeated with various tetraalkylammonium cations and a notable change in the voltammetric response can be observed (Fig. 1c and Figs. S2 and S3). With the HOPG WE, a cathodic peak current becomes apparent at *ca.* −2.0 V vs. $Ag/AgClO_4$. This is associated with the intercalation of the tetraalkylammonium cation and subsequent formation of some GIC [22]. It is thought that the GIC is stabilised by the neighbouring graphene sheets. As in the Li^+ intercalation case, the anodic peak is also visible.

With the Pt WE it can be clearly seen that all three tetraalkylammonium ions yield no specific current processes on the reductive scan, other than a general increase of background current (black line). This is due to reduction/decomposition of the electrolyte and/or solvent [37] and has been treated as the negative limit of the workable potential window. There is no oxidative response visible on the reverse scan in the Pt electrode case, which indicates that tetraalkylammonium reduction is irreversible on the Pt surface under these conditions [37,38], therefore the observation of the anodic current in the case of the graphite electrode implies that the reduction products are stabilized by intercalation.

In the HOPG cases, (Fig. 1, Figs. S2 and S3) it should also be noted that successive scans do not yield repeatable current responses. This is due to the continually changing working electrode structure, as the HOPG is seen to expand and fan out as a result of structurally-irreversible intercalation/de-intercalation. The difference between the absolute currents of the platinum wire and the HOPG electrode is attributed to the difference in the working area of the electrode i.e. the area of the electrode exposed to the electrolyte. This was confirmed by fabrication of a graphite rod with a 3 mm working

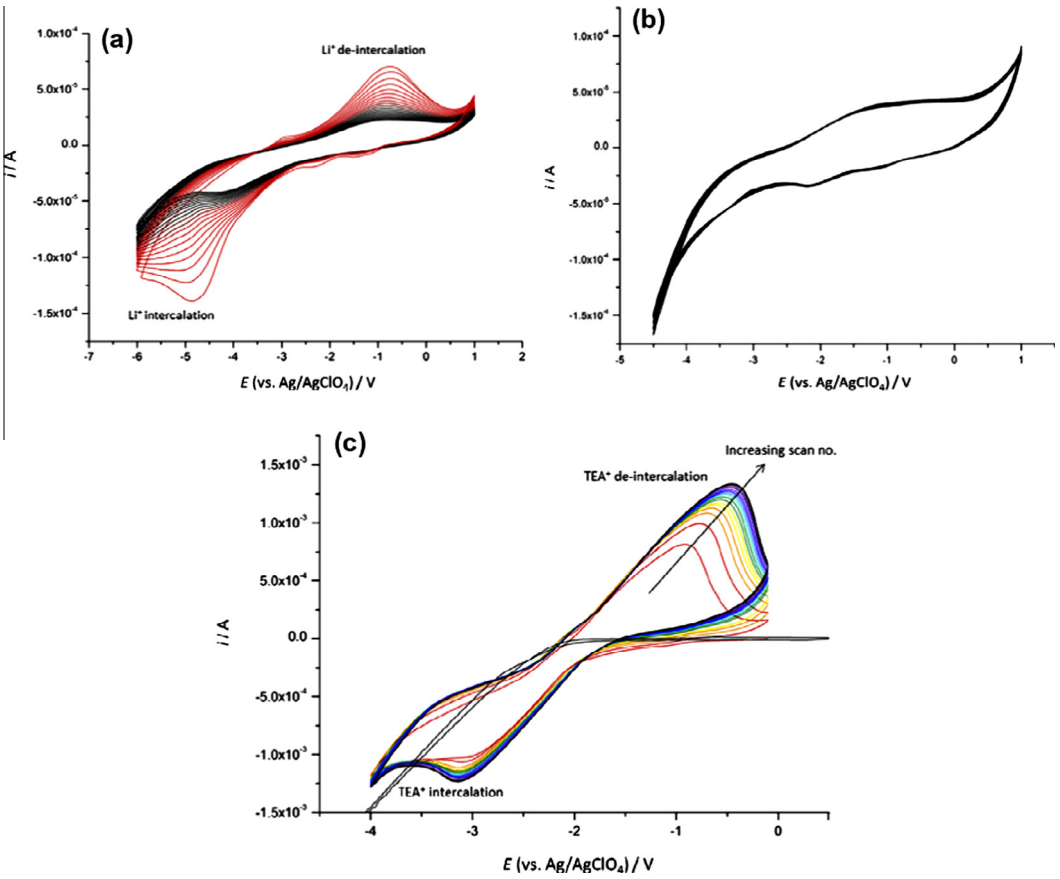

Fig. 1 – CVs of HOPG WE, Pt CE in 0.1 M electrolyte in NMP recorded at scan rates of 0.1 V s^{-1} at 25 °C, (a) and (b) Li^+ intercalation from $LiBF_4$, (c) TEA^+ intercalation from $TEABF_4$ (Pt WE, black line). HOPG working electrode measured approximately 3 × 10 × 0.5 mm. (A colour version of this figure can be viewed online.)

diameter compared to a glassy carbon (GC) electrode of the same diameter. Both electrodes displayed equal absolute currents at −4 V vs. $Ag/AgClO_4$ (Fig. S4).

3.2. *HOPG intercalation and subsequent expansion*

The potentials observed in the CV response were used to define those set in chronoamperometric mode to control the intercalation processes. From this, a potential of −5.0 V was applied to the HOPG working electrode for 6000 s and the degree of expansion recorded. Here −5.0 V was applied, rather than −4.0 V, so that the potential applied exceeded the intercalation peak and ensured complete intercalation of the cationic species. The HOPG expansion rate was found to be twice as fast with TBA as with TEA (Fig. 2a–c). Visual expansion of the HOPG electrode was not observed with TMA over these time periods. With TEA and TBA, the electrode was found to fan out from the point of contact with the tweezers and electrode fracture often began to occur after 6000 s (Fig. 2d and e).

Fig. 2f shows the effect of TBA intercalation on the HOPG structure with distortion of the planes by micron-sized pores, created by the intercalation of TBA and TEA. The planes do not separate uniformly, which may be due to the bulky nature of the cations and/or the Van der Waals forces holding the planes together. Fig. 2g shows a portion of HOPG which has been submerged in the electrolyte (right hand side) compared to a portion not exposed to the electrolyte (left hand side). The planes can be clearly seen to be exfoliating as a result of exposure to the electrolyte.

3.3. *HOPG expansion–X-ray Diffraction (XRD)*

XRD analysis was conducted on fresh HOPG (Fig. 3a) and intercalated HOPG samples (Fig. 3b) to investigate the degree of intercalation with respect to inter-planar gallery expansion. Heavily expanded samples resulted in diffraction patterns with a large broad peak in the $2\theta = 10–25°$ region, indicating an almost complete loss of structural crystallinity created from the intercalated species (Fig. S5), however samples expanded for less than 3000 s retained sharp peaks in their diffraction patterns. For pristine HOPG, the (002) peak at $2\theta = 26°$ corresponds to the inter-planar spacing of HOPG and has a calculated d-spacing of 0.335 nm, as expected (Fig. 3a). It can be seen that the TEA intercalated HOPG sample developed peaks in the $2\theta = 10–25°$ region in comparison to the same region for as prepared HOPG, which appeared featureless. These new peaks correspond to a range of new d spacings (0.375, 0.387, 0.453, 0.531 and 0.663 nm) shown in the inset of Fig. 3b, noting that 0.663 nm is a similar size to the TEA cation diameter (0.674 nm) [35]. The non-uniform expansion of the galleries is also reflected in the broadening

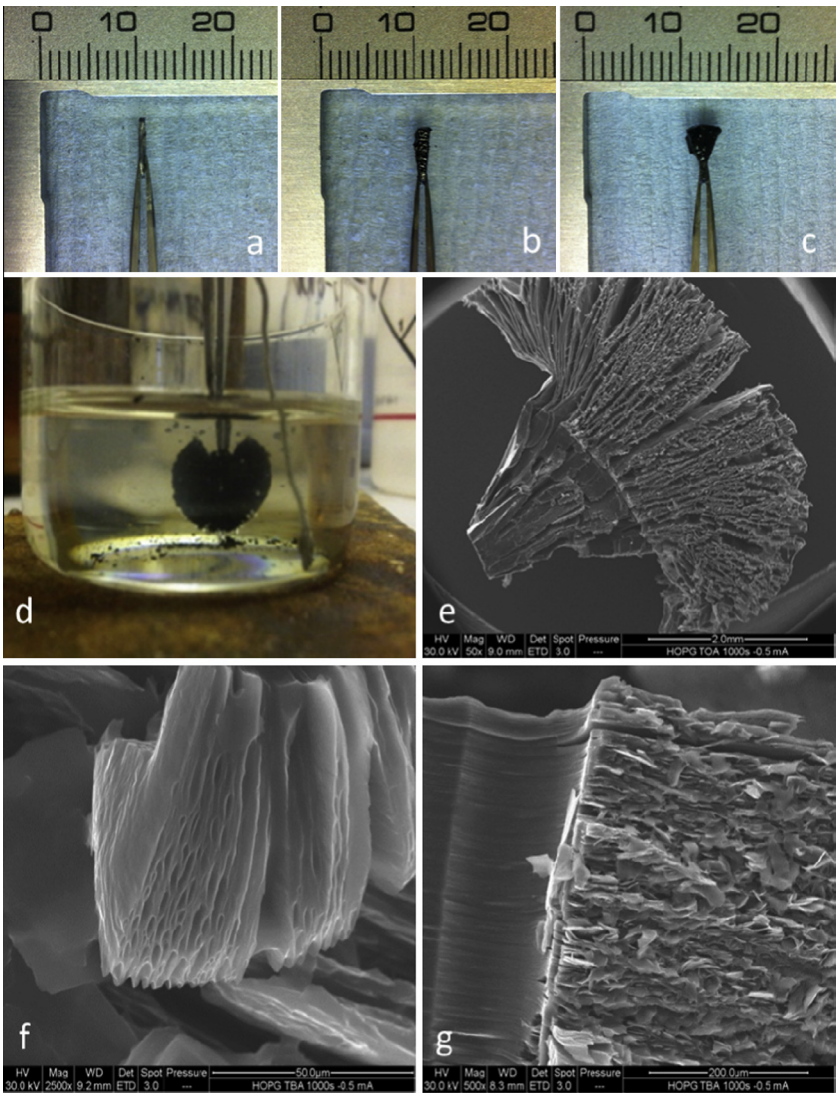

Fig. 2 – (a) Photographs of as prepared HOPG, (b) HOPG expansion after 1000 s TEA^+ intercalation, (c) HOPG expansion after 1000 s TBA^+ intercalation, (a–c scale in mm) (d) HOPG expansion after 10,000 s TBA^+ intercalation, (e) SEM image of HOPG expansion after 6000 s TBA intercalation, (f) SEM image showing micron sized pores in HOPG after TBA intercalation, (g) SEM image showing selective exfoliation of HOPG electrode: the point on a HOPG electrode that was held by tweezers (left hand side) whilst the rest of the electrode (right hand side) was submerged. (A colour version of this figure can be viewed online.)

and intensity decrease of the (002) peak (and subsequent (004) and (006) peaks) and it is thought this arises as a result of the flexibility of the TEA cation.

Additionally, a regular peak at $2\theta = 30°$ appeared on all expanded samples and was prominent enough also to appear as overtones. This peak corresponds to galleries with smaller *d* spacings than 0.335 nm (gallery contraction) and may be attributed to planes narrowing as a result of neighbouring planes separating.

3.4. *HOPG exfoliation*

HOPG electrochemical expansion was not accompanied by observable electrode exfoliation and no visible flakes were found on alumina membranes following filtration of the electrolyte solution. Expanded HOPG was transferred to a vial of pure NMP for 6 h sonication, at approximately 100 W to facilitate HOPG exfoliation. The vials were centrifuged (13,500 rpm for 30 min), filtered and flakes analysed *via* Raman spectroscopy.

Fig. 4 shows the Raman 2D bands associated with three typical flakes obtained *via* TBA intercalation. Freshly cleaved HOPG can be seen to produce the characteristic Raman 2D signal of graphite, as expected. The TBA derived flakes show a shift in the 2D band and are estimated to be between 2 and 5 layers in thickness, as indicated by the symmetrical Lorentzian shape of the 2D band at *ca.* 2660 cm^{-1} [39]. This is in contrast to the 2D band associated with bulk graphite (>10 layers).

HOPG has been found not to exfoliate directly while it is physically connected to the electrochemical cell. An additional sonication stage is needed to provide the energy required to split the layers completely. However, it has been found that an electrochemical intercalation pre-step can

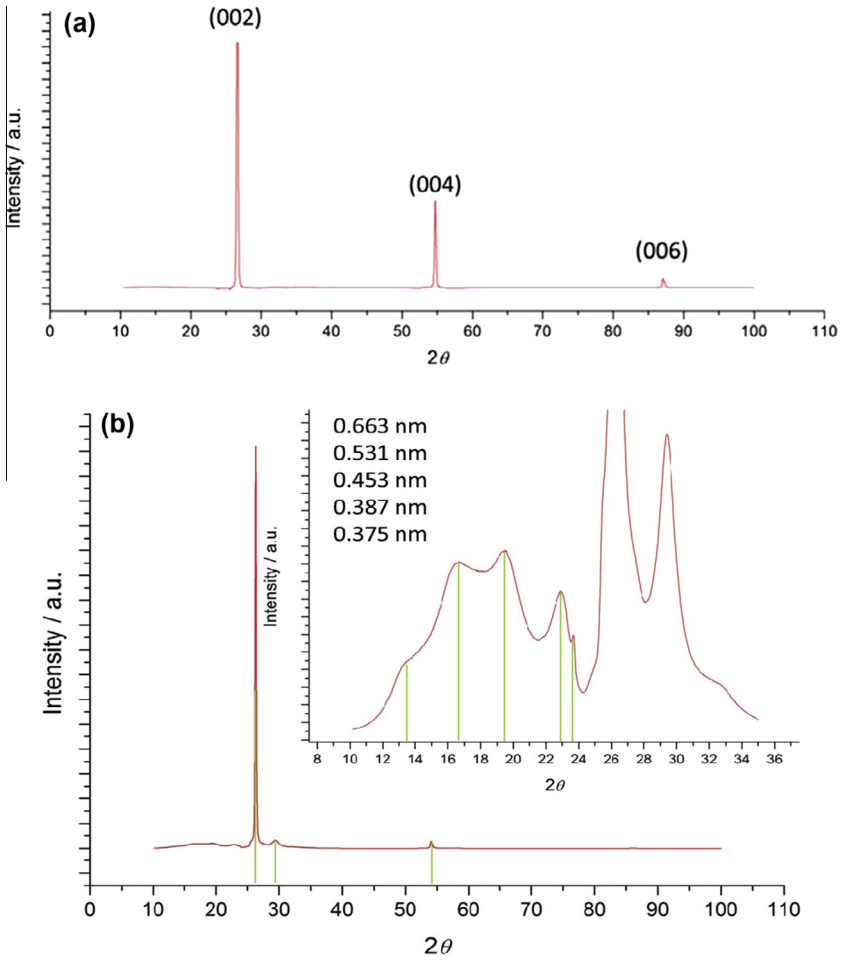

Fig. 3 – XRD pattern for (a) as prepared HOPG, (b) HOPG after intercalated with TEA^+ for 2000 s, inset in (b) is a magnified view of the small angle peaks in (b). (A colour version of this figure can be viewed online.)

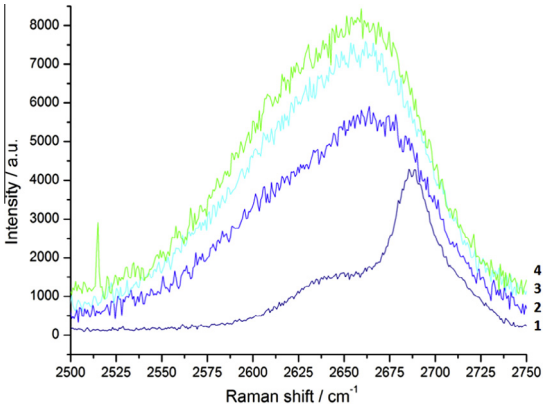

Fig. 4 – Comparative Raman spectra of as prepared HOPG and exfoliated flakes: Line 1: as prepared HOPG; Lines 2–4: typical 2D signals acquired from TBA^+ intercalated HOPG for 6000 s at −5.0 V followed by 6 h sonication. (A colour version of this figure can be viewed online.)

facilitate the exfoliation of HOPG into fewer layers. The electrode connection and/or the large HOPG grain size of 0.5–1.0 mm (*cf.* graphite rod grain size 2–5 μm), inherently prevent the complete exfoliation of the material. The diffusion coefficient of Li^+ into HOPG has been found to be on the order of 10^{-7} cm^2 s^{-1} [34], which would require complete exfoliation times exceeding *ca.* 30 h due to the relatively large grain sizes.

As a comparison, it was noted that as prepared HOPG, sonicated for 6 h at approximately 100 W, displayed no visible exfoliation products.

3.5. *Graphite rod exfoliation*

The same initial electrochemical procedure was repeated using a graphite rod electrode. CVs were run (Fig. S4) and gave equal absolute anodic currents (−1.4 mA) to the comparable HOPG electrode. It was found that the graphite rod exfoliated without the need for sonication when intercalating TMA, TEA and TBA. Initially, −5 V was applied to the graphite rod for a total period of 6 h. Direct electrode exfoliation was observed after as little as two CV cycles and, as shown in Fig. 5, exfoliate could be seen clearly falling as a stream from the graphite cathode over a period of 60,000 s. The visible exfoliate ranged from dark graphite-like fragments to barely visible particles. Fig. S6 shows the same experiments with $LiBF_4$ and it can be seen that no exfoliation of the graphite rod occurs even after prolonged intercalation times, although a grey precipitate was seen on the electrode (Fig. S7).

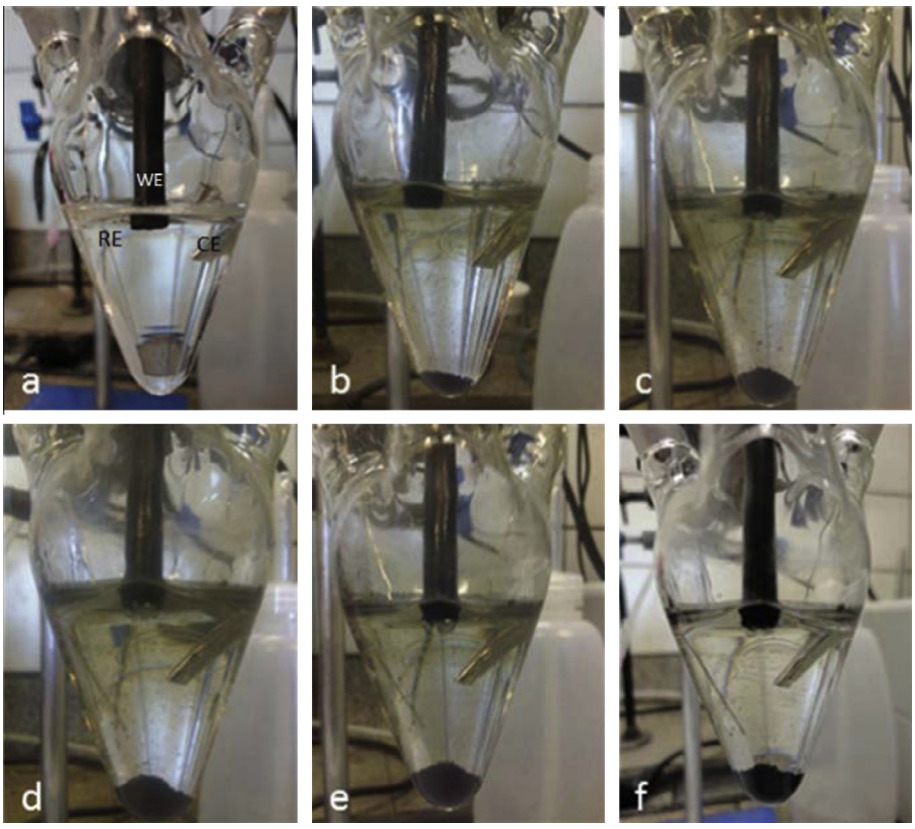

Fig. 5 – Successive intercalation every 10,000 s showing successful electrochemical exfoliation of a graphite rod using TEA^+. Intercalation at −5 V applied for a total of 60,000 s. Pt CE and Pt RE. Exfoliate can be seen in the bottom of the cell. (a) 10,000 s, (b) 20,000 s, (c) 30,000 s, (d) 40,000 s, (e) 50,000 s and (f) 60,000 s. (A colour version of this figure can be viewed online.)

It was found that graphite rod exfoliation by TMA occurred at a minimum potential of −2.4 V (vs. $Ag/AgClO_4$). Potentials of −2.4 V and −2.6 V were applied to the graphite rod for 24 h using $TMAClO_4$ as electrolyte. Graphitic exfoliate was visible to the eye and the resulting dispersions, having been left to stand for 48 h, were photographed (Fig. 6). A small aliquot of the supernatant was removed and pipetted onto a Si/SiO_2 wafer for AFM analysis. The samples were heated to 200 °C to ensure complete solvent evaporation. It was assumed that any few layer materials would disperse readily in the NMP and the heavier graphite-like material would settle spontaneously, consequently centrifugation was not performed on these samples.

AFM analysis of exfoliate dropped directly onto Si/SiO_2 shows isolated graphene flakes, Fig. 7a. A larger area scan, Fig. 7b, illustrates the distribution of graphene flake sizes. The flakes are of a variety of shapes and sizes but, as the height profiles of Fig. 7c and e show, they are of fairly uniform thickness.

We believe the reasons for the narrow distribution of flake heights result from intercalation occurring at best every 2–5 layers, due to the size and relative inflexibility of the TMA cation. This size exclusion effect prevents intercalation between every pair of neighbouring graphene sheets and thus acts as a barrier to the production of thinner flake material. Because of this, thinner exfoliated material was not present in the AFM analysis. Additionally, the 48 h dispersion resting time prior to AFM allows thicker graphitic material to settle and is not included in the analysis leaving the thinnest flakes (observed) in dispersion.

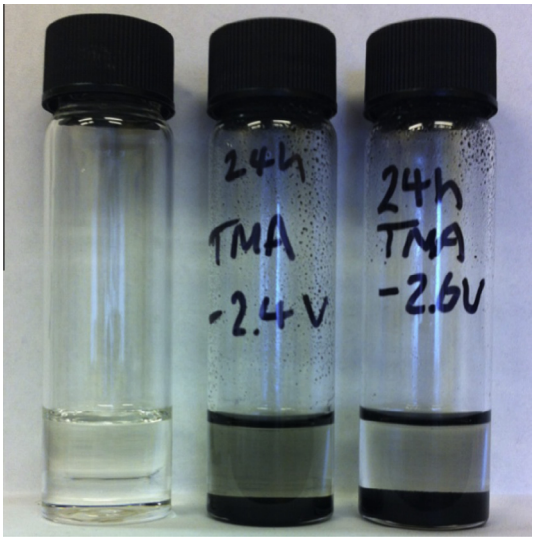

Fig. 6 – Fresh NMP (left), dispersions of graphite rod after 12 h intercalation of TMA at −2.4 V (centre) and −2.6 V (right), which in both cases had then been left to rest for 48 h. (A colour version of this figure can be viewed online.)

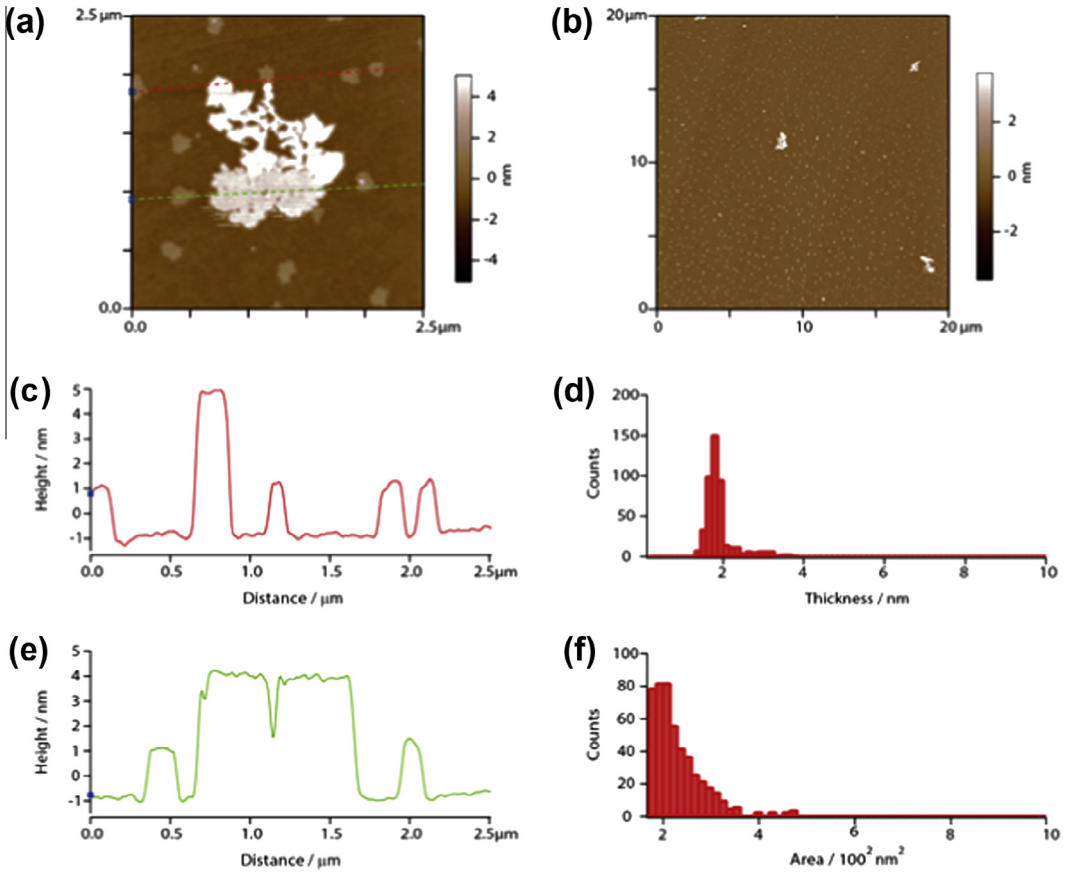

Fig. 7 – AFM images of flakes prepared *via* 12 h TMA intercalation (−2.4 V) and subsequent exfoliation of the graphite rod. (a) Zoom in of representative 2.5 µm × 2.5 µm area showing AFM traces, (b) micrograph of typical 20 × 20 µm area of Si/SiO_2 substrate supporting flakes, (c) corresponding height measurements of red traced path in (a), (d) flake thickness (nm) distribution of 456 graphene islands, (e) corresponding height measurements of green traced path in (a), (f) flake area distributions (m^2, $(20 \times 10^{-15}\ m)^{1/2}$ corresponds to 140 nm) of 456 graphene islands. (A colour version of this figure can be viewed online.)

Statistical analysis of the roughly 500 graphene flakes visible in this image shows that the typical thickness of the graphene flakes is around 1.8 nm, Fig. 7d. Most of the graphene flakes have a diameter of 100–200 nm (corresponding to an area of 1×10^4–4×10^4 nm^2), Fig. 7f. A few larger, micrometre size flakes are observed, but these are typically thicker. Flake counting revealed an estimated yield of *ca.* 16 flakes per square micron.

The concentration of the few-layer graphene dispersion (TMA exfoliated, 12 h) was estimated to be on the order of 0.01 mg mL^{-1} as calculated *via* UV–Vis absorption and the use of the Lambert–Beer relationship. The dispersion was placed in a quartz cuvette with a 2 mm cell length and the absorbance measured at 660 nm vs. a reference solution of 0.1 M $TMAClO_4$ electrolyte in NMP. The absorption coefficient, 2.46×10^3 L g^{-1} m^{-1}, was the value previously quoted by Coleman et al. [15] for few layer graphene dispersions (<5 layers) and an absorbance of 0.058 was recorded, corresponding to a concentration of 11.8 µg mL^{-1}.

Fig. 8a shows the full Raman spectra acquired from the graphite rod prior to electrochemical intercalation and from a TBA exfoliated flake. It can be seen that the 2D band has shifted from *ca.* 2670 cm^{-1} to *ca.* 2650 cm^{-1}. Additionally, there is a slight negative shift in the G peak by approximately 20 cm^{-1}. Both these shifts are attributed to thinner flake graphene material, estimated to be between 2 and 5 layers. The I_{2D}/I_G value decreases from *ca.* 0.68 to *ca.* 0.64. This small value is thought to be a result of the relatively large D peaks, since it has been reported that an increasing I_D/I_G, resulting from edge defects, can have an inverse effect on the ratio I_{2D}/I_G [40]. Additionally, the D peak at *ca.* 1350 cm^{-1} is often present. The presence of this D peak is thought to be a function of the edge defects present on the flakes, rather than a loss of sp^2 bonding, since flake lateral sizes were typically smaller than the laser spot diameter (*ca.* 2 µm). It was thus not possible to exclude all of the flake edges from the analysis and a D peak was always observed.

Fig. 8b shows the 2D signals acquired from three different flakes obtained from 12 h TBA intercalation. Again it can be seen that the 2D band position has moved from *ca.* 2670 cm^{-1} to *ca.* 2650 cm^{-1} for the flakes exfoliated from the original graphite rod.

Finally, to probe the degree of flake functionalisation in the electrochemical procedure, XPS was conducted on exfoliated flakes as prepared *via* graphite rod exfoliation (Fig. 9a–d). The exfoliated flakes were washed with ethanol/pure NMP and

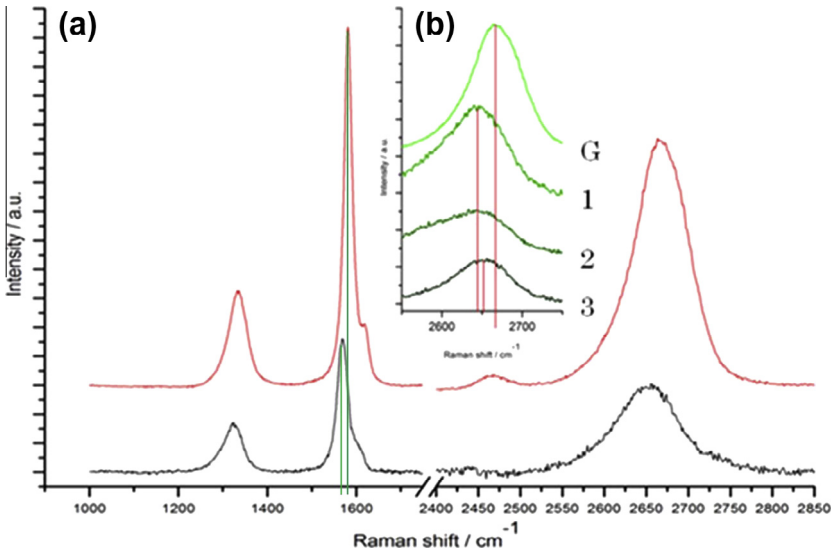

Fig. 8 – (a) Raman spectra of graphite rod pre intercalation (red) and exfoliate (black), (b) Raman 2D signals from as prepared graphite rod (G) and three typical exfoliated flakes (1, 2, 3). (A colour version of this figure can be viewed online.)

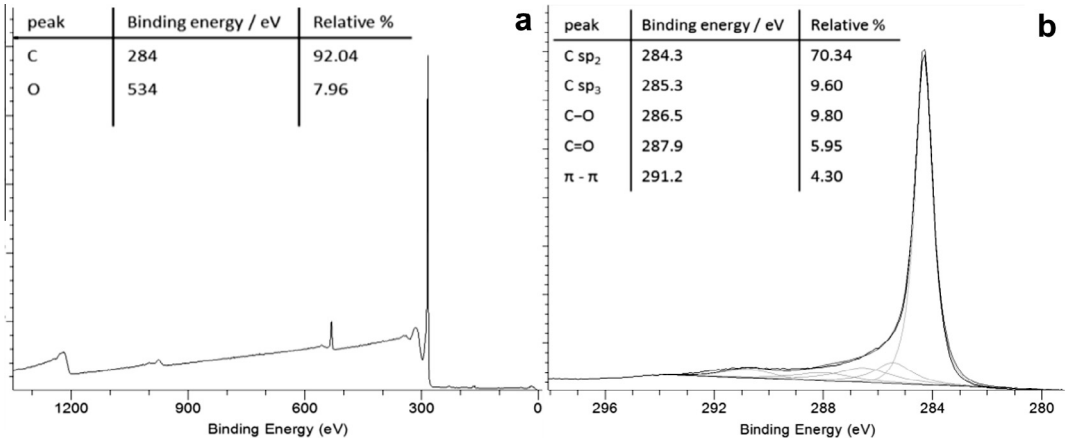

Fig. 9 – (a) XPS survey spectrum and (b) C1s spectrum of graphite rod exfoliation.

oven dried. Flakes were stored in sealed boxed (containing air) directly after isolation for 1 week until XPS was available. The original graphite rod was ball milled and also analysed with XPS as a powder. The XPS data collected from the exfoliate powder showed that the sample consisted of *ca.* 8% oxygen and *ca.* 92% carbon (Fig. 9a). Analysis of the ball milled graphite rod, prior to any electrochemical treatment, was found to consist of 5.4% oxygen (Fig. S8c). This <3% increase in oxygen content may have been introduced during the washing procedure or from atmospheric exposure during the waiting time prior to XPS analysis, since no oxidative process was involved in the electrochemical procedure. Closer inspection of the C1s peak (Fig. 9b) shows the peak can be fitted reasonably well to five Lorentzian functions corresponding to five different carbon states of different binding energies. The main peak at 284.3 eV corresponds to sp^2 carbon and accounts for *ca.* 70% of the carbon peak and a smaller peak at 285.3 eV indicates a degree of sp^3 carbon, accounting for 9.6% of the C1s peak. The two carbon–oxygen peaks (C–O and C=O) are found at 286.5 eV and 287.9 eV, respectively, and have a total contribution of 15.95% of the C1s peak [14,23,41–43]. Finally a π–π^* resonance peak is observed at 291.2 eV and is associated with graphitic materials. Additionally, XPS showed a negligible amount of nitrogen on the sample (Fig. S8a) [43].

4. Conclusions

Herein we present a controlled method for the production of few-layer graphene. It is thought that HOPG, although structurally ideal for exfoliation, presents problems due to the nature of the electrode set up. For HOPG, TBA was found to be the most effective cation for electrode expansion, followed by TEA. This can be explained by the respective cationic diameters: 0.558 nm (TMA), 0.674 nm (TEA), and 0.826 nm (TBA) [35,36] which are slightly larger than the interlayer spacing of HOPG: 0.354 nm. Although TBA is almost three times the size of the graphene interplanar spacing, the intercalation is permitted due to flexibility of the alkyl groups and the ability of the TBA ion to flatten between the graphene sheets [22]. Lithium tetrafluoroborate $LiBF_4$ was also used as an additional

comparative electrolyte, with a cationic diameter of 0.146 nm [35,36]. It should be highlighted that Li^+ containing electrolytes did not result in exfoliation of HOPG or the graphite rod which strongly suggests the cationic diameter is a key factor in the successful exfoliation.

Electrode expansion was significantly more noticeable with an HOPG electrode than with a graphite rod electrode and it is suspected that HOPG's affinity for expansion is a result of its high anisotropy, since the crystallographic orientation of HOPG is extremely uniform in comparison to the synthesized rods. The intercalated tetraalkylammonium cations are not solely able to expand the HOPG electrode to breaking point due to HOPG's high crystal orientation and hence sonication is necessary to overcome this additional binding energy.

Alternatively, it is shown that electrochemical intercalation of tetraalkylammonium cations into a graphite rod directly yields few layer graphene (between 2 and 5 layers with TMA) and does not require any additional exfoliation step. This is due to the relatively random orientation of the graphite flakes in the graphite rod. The additional binding energy as a result of high crystallographic orientation, as seen in HOPG, is not present in the graphite rod and is reflected by the relative ease with which graphite rods exfoliate and the lack of observed expansion.

The XPS data acquired suggests that a 3% increase in the oxygen content is introduced at some stage during the procedure. Since it is unlikely that oxidative processes are occurring within the experimental potential region, the introduction of oxygen is suspected to arise as a result of the washing procedure, and subsequent handling, rather than during cathodic treatment of the graphite. It is believed that although the waiting time between flake isolation and flake characterization might have a small oxidizing effect on the flakes due to exposure to air, it is not thought to affect AFM results significantly.

Work remains to improve the calculated 11.8 $\mu g\,mL^{-1}$ concentration of few-layer graphene material in dispersion and to optimize the lateral flake sizes of the exfoliated graphene sheets, however flake quality appears to be acceptable (AFM deduced average size and thickness distributions: 100–200 nm and 1.8 nm respectively). The small flake sizes obtained with this method may be attributed to the small crystallite size of the graphite making up the rod (2–5 μm). Nonetheless, this single stage electrochemical route constitutes a viable option for the production of few-layer graphene due to its minimal energy requirements and relative ease of operation.

Acknowledgements

We thank the UK EPSRC for a studentship for A.J.C. and further financial support (Grant references EP/I005145/1 and EP/K016954/1). We thank Dr. Anders Barlow of the National EPSRC XPS Users Service (NEXUS), Newcastle University for assistance with XPS measurements.

Appendix A. Supplementary data

Supplementary data additional characterisation and experimental data associated with this article can be found, in the online version, at http://dx.doi.org/10.1016/j.carbon.2013.09.009.

REFERENCES

[1] Shih CJ, Vijayaraghavan A, Krishnan R, Sharma R, Han JH, Ham MH, et al. Bi- and trilayer graphene solutions. Nat Nanotechnol 2011;6(7):439–45.
[2] Gong L, Young RJ, Kinloch IA, Riaz I, Jalil R, Novoselov KS. Optimizing the reinforcement of polymer-based nanocomposites by graphene. ACS Nano 2012;6(3):2086–95.
[3] Novoselov KS, Geim AK, Morozov SV, Jiang D, Zhang Y, Dubonos SV, et al. Electric field effect in atomically thin carbon films. Science 2004;306(5696):666–9 [October 22, 2004].
[4] Sutter PW, Flege J-I, Sutter EA. Epitaxial graphene on ruthenium. Nat Mater 2008;7(5):406–11.
[5] Reina A, Jia X, Ho J, Nezich D, Son H, Bulovic V, et al. Large area, few-layer graphene films on arbitrary substrates by chemical vapor deposition. Nano Lett 2008;9(1):30–5.
[6] Lee S, Lee K, Zhong Z. Wafer scale homogeneous bilayer graphene films by chemical vapor deposition. Nano Lett 2010;10(11):4702–7.
[7] Castro-Neto AH, Guinea F, Peres NMR, Novoselov KS, Geim AK. The electronic properties of graphene. Rev Mod Phys 2009;81(1):109–62.
[8] Lopes dos Santos JMB, Peres NMR, Castro Neto AH. Graphene bilayer with a twist: electronic structure. Phys Rev Lett 2007;99(25):256802.
[9] Liu LX, Zhou HL, Cheng R, Yu WJ, Liu Y, Chen Y, et al. High-yield chemical vapor deposition growth of high-quality large-area AB-stacked bilayer graphene. ACS Nano 2012;6(9):8241–9.
[10] Hummers WS, Offeman RE. Preparation of graphitic oxide. J Am Chem Soc 1958;80(6):1339.
[11] Ang PK, Wang S, Bao Q. High-throughput synthesis of graphene by intercalation–exfoliation of graphite oxide and study of ionic screening in graphene transistor. ACS Nano 2009;3(11):3587–94.
[12] Gómez-Navarro C, Weitz RT, Bittner AM, Scolari M, Mews A, Burghard M, et al. Electronic transport properties of individual chemically reduced graphene oxide sheets. Nano Lett 2007;7(11):3499–503.
[13] Allen MJ, Tung VC, Kaner RB. Honeycomb carbon: a review of graphene. Chem Rev 2009;110(1):132–45.
[14] Wang J, Manga KK, Bao Q, Loh KP. High-yield synthesis of few-layer graphene flakes through electrochemical expansion of graphite in propylene carbonate electrolyte. J Am Chem Soc 2011;133(23):8888–91.
[15] Hernandez Y, Nicolosi V, Lotya M, Blighe FM, Sun Z, De S, et al. High-yield production of graphene by liquid-phase exfoliation of graphite. Nat Nanotechnol 2008;3(9):563–8.
[16] Lu J, Loh KP. One-pot synthesis of fluorescent carbon nanoribbons, nanoparticles, and graphene by the exfoliation of graphite in ionic liquids. ACS Nano 2009;3(8):2367–75.
[17] Liu WW, Wang JN. Direct exfoliation of graphene in organic solvents with addition of NaOH. Chem Commun 2011;47(24):6888–90.
[18] Wang X, Fulvio PF, Baker GA, Veith GM, Unocic RR, Mahurin SM, et al. Direct exfoliation of natural graphite into micrometre size few layers graphene sheets using ionic liquids. Chem Commun 2010;46(25):4487–9.
[19] Morales GM, Schifani P, Ellis G, Ballesteros C, Martínez G, Barbero C, et al. High-quality few layer graphene produced by electrochemical intercalation and microwave-assisted expansion of graphite. Carbon 2011;49(8):2809–16.

[20] Zhou M, Tang J, Cheng Q, Xu GJ, Cui P, Qin LC. Few-layer graphene obtained by electrochemical exfoliation of graphite cathode. Chem Phys Lett 2013;572:61–5.
[21] Liu N, Luo F, Wu H, Liu Y, Zhang C, Chen J. One-step ionic-liquid-assisted electrochemical synthesis of ionic-liquid-functionalized graphene sheets directly from graphite. Adv Funct Mater 2008;18(10):1518–25.
[22] Sirisaksoontorn W, Adenuga AA, Remcho VT, Lerner MM. Preparation and characterization of a tetrabutylammonium graphite intercalation compound. J Am Chem Soc 2011;133(32):12436–8.
[23] Buqa H, Blyth RIR, Golob P, Evers B, Schneider I, Santis Alvarez MV, et al. Negative electrodes in rechargeable lithium ion batteries—influence of graphite surface modification on the formation of the solid electrolyte interphase. Ionics 2000;6(3–4):172–9.
[24] Bernard G, Simonet J. Irreversible cathodic behavior of graphite in the presence of some mixtures of onium salts. J Electroanal Chem Interfacial Electrochem 1979;96(2):249–53.
[25] Simonet J, Lund H. Electrochemical behaviour of graphite cathodes in the presence of tetraalkylammonium cations. J Electroanal Chem Interfacial Electrochem 1977;75(2):719–30.
[26] Akçay M. Characterization and adsorption properties of tetrabutylammonium montmorillonite (TBAM) clay: thermodynamic and kinetic calculations. J Colloid Interface Sci 2006;296(1):16–21.
[27] Golub AS, Zubavichus YV, Slovokhotov YL, Novikov YN, Danot M. Layered compounds assembled from molybdenum disulfide single-layers and alkylammonium cations. Solid State Ionics 2000;128(1–4):151–60.
[28] Besenhard JO, Möhwald H, Nickl JJ. Electronic conductivity and structure of DMSO-solvated A+- and NR4+-graphite intercalation compounds. Carbon 1980;18(6):399–405.
[29] Besenhard JO, Fritz HP. Cathodic reduction of graphite in organic solutions of alkali and NR4+ salts. J Electroanal Chem Interfacial Electrochem 1974;53(2):329–33.
[30] Besenhard JO. The electrochemical preparation and properties of ionic alkali metal- and NR4-graphite intercalation compounds in organic electrolytes. Carbon 1976;14(2):111–5.
[31] Zhong YL, Swager TM. Enhanced electrochemical expansion of graphite for in situ electrochemical functionalization. J Am Chem Soc 2012;134(43):17896–9.
[32] Breant MB, Buisson C, Dupin M, Rebattu J. Electrochemie dans la N-methylpyrollidone. Bulletin De La Societe Chimique De France 1968;12(810):5065.
[33] Pollak E, Geng B, Jeon K-J, Lucas IT, Richardson TJ, Wang F, et al. The interaction of Li+ with single-layer and few-layer graphene. Nano Lett 2010;10(9):3386–8.
[34] Persson K, Sethuraman VA, Hardwick LJ, Hinuma Y, Meng YS, van der Ven A, et al. Lithium diffusion in graphitic carbon. J Phys Chem Lett 2010;1(8):1176–80.
[35] Osakai T, Ebina K. Non-Bornian theory of the Gibbs energy of ion transfer between two immiscible liquids. J Phys Chem B 1998;102(29):5691–8.
[36] Stephenson MJ, King AJ, Holmes SM, Dryfe RAW. Size selective and volume exclusion effects on ion transfer at the silicalite modified liquid–liquid interface. J Phys Chem B 2005;109(41):19377–84.
[37] Simonet J, Astier Y, Dano C. On the cathodic behaviour of tetraalkylammonium cations at a platinum electrode. J Electroanal Chem 1998;451(1–2):5–9.
[38] Dahm CE, Peters DG. Electrochemical reduction of tetraalkylammonium tetrafluoroborates at carbon cathodes in dimethylformamide. J Electroanal Chem 1996;402(1–2):91–6.
[39] Ferrari AC, Meyer JC, Scardaci V, Casiraghi C, Lazzeri M, Mauri F, et al. Raman spectrum of graphene and graphene layers. Phys Rev Lett 2006;97(18):187401.
[40] Das A, Chakraborty B, Sood AK. Raman spectroscopy of graphene on different substrates and influence of defects. Bull Mater Sci 2008;31(3):579–84.
[41] Wang Y, Sun H, Zhang R, Yu S, Kong J. Large scale templated synthesis of single-layered graphene with a high electrical capacitance. Carbon 2013;53:245–51.
[42] Yang D, Velamakanni A, Bozoklu G, Park S, Stoller M, Piner RD, et al. Chemical analysis of graphene oxide films after heat and chemical treatments by X-ray photoelectron and micro-Raman spectroscopy. Carbon 2009;47(1):145–52.
[43] Phaner-Goutorbe M, Sartre A, Porte L. Soft oxidation of graphite studied by XPS and STM. Microsc Microanal 1994;5(4–6):283–90.